npj | Quantum Information

www.nature.com/npjqi

ARTICLE OPEN

Check for updates

Detecting non-Markovianity via quantified coherence: theory and experiments

Kang-Da Wu[1,2], Zhibo Hou[1,2], Guo-Yong Xiang[1,2]✉, Chuan-Feng Li[1,2], Guang-Can Guo[1,2], Daoyi Dong[3] and Franco Nori[4,5]

The dynamics of open quantum systems and manipulation of quantum resources are both of fundamental interest in quantum physics. Here, we investigate the relation between quantum Markovianity and coherence, providing an effective way for detecting non-Markovianity based on the quantum-incoherent relative entropy of coherence ($\mathcal{QI}$ REC). We theoretically show the relation between completely positive (CP) divisibility and the monotonic behavior of the $\mathcal{QI}$ REC. Also we implement an all-optical experiment to demonstrate that the behavior of the $\mathcal{QI}$ REC is coincident with the entanglement shared between the system and the ancilla for both Markovian and non-Markovian evolution; while other coherence-based non-Markovian information carriers violate monotonicity, even in Markovian processes. Moreover, both theoretically and experimentally, we show that non-Markovianity enhances the ability of creating coherence on an ancilla. This is the first experimental study of the relation between dynamical behavior of the $\mathcal{QI}$ REC and the phenomenon of information backflow. Our methods for detecting non-Markovianity are applicable to general quantum evolutions.

npj Quantum Information (2020)6:55 ; https://doi.org/10.1038/s41534-020-0283-3

INTRODUCTION

Quantum resource theory[1] studies the transformation and conversion of information under certain constrains. The quantification and manipulation of various resources are of central interest in quantum information, quantum thermodynamics, and other fields of physics[2–5]. Recently, resource theories have inspired rigorous studies on the long-standing notions of non-classicality in localized systems, where the development of coherence theory has become a fundamental task[6–11].

Coherence is an intrinsically vulnerable resource, inevitably vanishing at macroscopic scales of space, time, and temperature[12–17]. This becomes apparent in the study of the dynamical behavior of such resource in the presence of dissipation, where the system is rarely isolated and usually loses its information due to its environment[18–27]. The problem of classifying memoryless dynamics and dynamics exhibiting memory effects has stimulated numerous investigations on the system-environment interaction. There are two main ideas: one idea, based on divisibility of the dynamical maps[28,29], is an analogy with the definition of classical stochastic processes; the other idea[30] demonstrates that the memory effects may be accompanied by an information backflow, which is reflected by the non-monotonic behavior of some physical quantities[30–43].

Rigorous studies on the dynamical behavior of quantified coherence in non-Markovian dynamics have recently attracted considerable attention[44–54]. Moreover, information quantifiers based on coherence and the extended coherence with an ancilla have been proposed, for measuring the degree of non-Markovianity. It is known that coherence behaves monotonically in an incoherent Markovian evolution. However, for a general Markovian evolution, the dynamical behavior of quantum coherence is not necessarily monotonic. Moreover, the coherence-based quantifier that evolves monotonically in a certain basis may not evolve monotonically in another basis. Thus, two basic requirements for an advantageous coherence-based non-Markovianity measures are: (a) it is applicable for general evolutions; (b) for a Markovian quantum evolution, the monotonicity of the dynamical behavior of the quantifier is independent of the choice of reference basis.

In this work, we introduce a new way for detecting non-Markovianity based on the $\mathcal{QI}$ REC of a bipartite system[55–57]. Theoretically, we show that Markovianity implies the monotonic behavior of both the $\mathcal{QI}$ REC and the steering-induced coherence (SIC, upper bounded by the $\mathcal{QI}$ REC)[56,57]. Experimentally, we compare our method with two existing approaches[47,48], and verify the advantages of our new method for characterizing non-Markovianity. Moreover, we experimentally detect non-Markovianity via the non-monotonic behavior of both the $\mathcal{QI}$ REC and the SIC, which is coincident with previous results based on entanglement. Our work links the resource theory of coherence to quantum Markovianity.

RESULTS

Quantum Markovianity

In general, quantum evolution can be characterized by a family of one-parameter dynamical maps $\{\Lambda_{t,0}\}$, which is completely positive and trace preserving (CPTP) for any $t > 0$, i.e., a legitimate quantum operation that maps the initial quantum state to the state at time t and we assume that the inverse $\Lambda_{t,0}^{-1}$ exists for all time $t > 0$. Thus, for any $t > s > 0$, we can write the dynamical map for any t into a composition

$$\Lambda_{t,0} = \Lambda_{t,s}\Lambda_{s,0}. \quad (1)$$

However, even though Λ_t^{-1} is well-defined and $\Lambda_{t,0}$, $\Lambda_{s,0}$ are completely positive (CP), the map $\Lambda_{t,s}$ does not need to be CP. If

[1]CAS Key Laboratory of Quantum Information, University of Science and Technology of China, 230026 Hefei, China. [2]CAS Center For Excellence in Quantum Information and Quantum Physics, University of Science and Technology of China, 230026 Hefei, China. [3]School of Engineering and Information Technology, University of New South Wales, Canberra, ACT 2600, Australia. [4]Theoretical Quantum Physics Laboratory, RIKEN Cluster for Pioneering Research, Wako-shi, Saitama 351-0198, Japan. [5]Physics Department, University of Michigan, Ann Arbor, MI 48109-1040, USA. ✉email: gyxiang@ustc.edu.cn

for any $t > s > 0$, $\Lambda_{t,s}$ is CP, then the family of dynamical maps is said to be CP divisible. This leads to the definition of quantum Markovianity, providing a mathematical characterization of a map describing a memoryless evolution as a composition of physical maps. In this paper we adopt CP divisibility as the essential property of quantum Markovianity.

A measure for non-Markovianity, proposed in ref. [40], is based on the idea that Markovian dynamics leads to a monotonic decrease of the entanglement between the open system and an isomorphic ancilla system; whereas non-Markovian dynamics induces a temporary increase of the entanglement. In our experiment we use this result for identifying whether the process is non-Markovian.

Quantum-incoherent relative entropy of coherence

A quantum resource theory (QRT) has several indispensable ingredients, including: constraints, states which contain no resource, and the measure of how much resource a state possesses. The constraints, known as free operations, in a QRT are the permissible operations. Because they do not encompass all physical processes that quantum mechanics allows, only certain physically realizable states of a quantum system can be prepared. These states are often referred to as free states, which is the set of all shapes that can be generated without any cost by a compass and a ruler (free operations). In the following, let us first briefly recall some basic information about free states and free operations in coherence theory.

In the resource theory of coherence, an orthogonal basis $\{|i\rangle\}$ is considered classical. Any mixture of such states

$$\chi = \sum_i p_i |i\rangle\langle i| \tag{2}$$

is termed incoherent, and thus is free.

Incoherent operations are naturally introduced as physical transformations that do not create coherence[6], which are the free operations in this context. These quantum operations Λ admit an incoherent Kraus decomposition

$$\Lambda[\rho] = \sum_i K_i \rho K_i^\dagger \tag{3}$$

with incoherent Kraus operators K_i, i.e., $K_i \mathcal{I} K_i^\dagger \subseteq \mathcal{I}$ for the set of incoherent states $\mathcal{I}$.

The amount of coherence for a general quantum state C quantifies how close it is from the set of incoherent states with respect to a given reference basis, i.e.,

$$C(\rho) = \min_{\chi \in \mathcal{I}} D(\rho \parallel \chi), \tag{4}$$

where D is a distance measure between two quantum states and $\mathcal{I}$ denotes the set of incoherent states. In this paper, we adopt the relative entropy as the measure for coherence C_r, i.e., $D(\rho \parallel \chi) = S(\rho \parallel \chi) = \mathrm{Tr}[\rho \log_2 \rho - \rho \log_2 \chi]$[58]. And the relative entropy of quantum coherence for a general quantum state ρ can be exactly evaluated as $C_r(\rho) = S(\Delta\rho) - S(\rho)$, where $S(\rho) = \mathrm{Tr}[\rho \log_2 \rho]$.

Strictly, C_r never increases under CPTP incoherent operations. However, when taking the advantage of assistance[55,59,60], one can increase C_r. Considering a bipartite system (Alice and Bob) sharing a quantum state described by ρ^{AB}, assume Alice can perform any local generalized measurement on her system and broadcast the outcomes to Bob. Then Bob can prepare more coherent states than his own states. In particular, the SIC[55–57], denoted as $\overline{C}_r^B(\rho^{AB})$, is defined as the maximal average coherence on Bob's side, with the assistance of Alice,

$$\overline{C}_r^B(\rho^{AB}) = \max_{\mathcal{M}_A} \sum_m p_m C_r(\rho_m^B), \tag{5}$$

where the optimization is taken over all local measurement $\mathcal{M}_A$ on Alice, and ρ_m is the state of Bob corresponding to the measurement outcome m of Alice.

The SIC captures the steerability from Alice to Bob, where coherence on Bob's side is demanded. Generally, the identification of the SIC needs a non-trivial optimization over all possible measurements of Alice. The upper bound of this quantity, the $\mathcal{QI}$ REC was recently introduced in refs [55,59]. For a bipartite state ρ^{AB}, the $\mathcal{QI}$ REC $C_r^{A|B}$ can be evaluated as

$$C_r^{A|B}(\rho^{AB}) \equiv \min_{\chi^{A|B} \in \mathcal{I}^{A|B}} S(\rho^{AB} \parallel \chi^{A|B}), \tag{6}$$

where $\chi^{A|B}$ denotes the bipartite states that are quantum-incoherent ($\mathcal{QI}$), i.e.,

$$\chi^{A|B} = \sum_i p_i \sigma_i^A \otimes |i\rangle\langle i|^B, \tag{7}$$

where σ_i^A represents an arbitrary quantum state, belonging to Alice. Equation (6) can also be evaluated as $C_r^{A|B}(\rho^{AB}) = S[\Delta^B(\rho^{AB})] - S(\rho^{AB})$, where Δ^B denotes a partial decoherence map on Bob's system. From the results in refs [55,59], we know that

$$C_r^{A|B}(\rho^{AB}) \geq \overline{C}_r^B(\rho^{AB}) \tag{8}$$

where ρ^{AB} stands for general bipartite mixed states. Note that the $\mathcal{QI}$ REC is a measure that is important in the resource theory of coherence. It is often related to the measure of quantum correlations, but is in general different from entanglement or correlation measure. And it also quantifies the upper bound for the ability of preparing the maximally coherent state $|+\rangle = \frac{1}{\sqrt{2}}(|0\rangle + |1\rangle)$ in asymptotic setting (see the Supplementary Information for details on the $\mathcal{QI}$ REC).

Previous results

Before describing our main results, we first introduce previous results (for non-Markovianity based on coherence measure that were proposed and tested very recently[44–54]). The previous results can be summarized as two main approaches, and both are applicable to detecting and quantifying the non-Markovianity of incoherent open system dynamics (IOSD).

Reference[47] utilizes the fact[6] that any coherence measure monotonically decreases under CPTP incoherent operations,

$$C[\Lambda(\rho)] \leq C(\rho), \tag{9}$$

for all incoherent operations Λ. Thus coherence can be used for detecting the non-Markovianity for quantum dynamics that preserves the set of incoherent states. This can be summarized in the following lemma[53],

- Lemma 1—Consider a quantum system ρ undergoing an IOSD characterized by $\Lambda_{t,0}$. Let ρ_s, ρ_t denote the quantum state after the evolution times s and t, respectively. The amount of quantum coherence decreases monotonically, i.e.,

$$C(\rho_t) \leq C(\rho_s), \forall t > s > 0, \tag{10}$$

  where C represents a coherence measure based on a contractive distance, such as relative entropy or l_1-norm[6].

In the Supplementary Information, we give a proof for this statement.

Reference[48] proposed an alternative non-Markovianity measure based on the relative entropy of coherence, which uses the whole relative entropy of coherence in an extended Hilbert space constituted by the open system (A) and its ancillary (B). This can be summarized as the second lemma[48],

- Lemma 2—Consider the aforementioned bipartite system described by ρ^{AB}, only Alice undergoes an IOSD characterized by $\Lambda_{t,0}$. Let ρ_s^{AB} and ρ_t^{AB} denote the overall quantum state after the evolution times s and t, respectively. The amount of

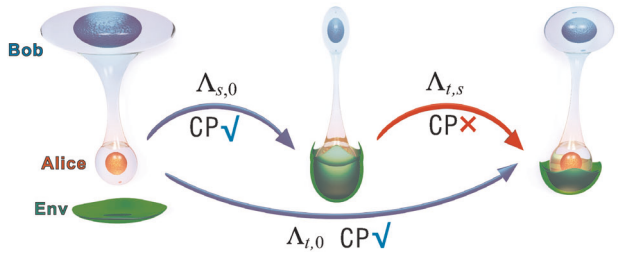

Fig. 1 Theoretical framework. Consider a bipartite system involving Alice (red, system) and Bob (blue, ancilla) with nonzero initial $\mathcal{QI}$ REC, which is shown by the larger volume of Bob. The environment is shown as green and can interact with Alice's system, while Bob is immune to the environment. Then Alice undergoes a quantum evolution characterized by a family of t-parameterized dynamical maps $\{\Lambda_t\}$. If the evolution is CP divisible, then the $\mathcal{QI}$ REC decreases monotonically. The CP divisibility also affects the ability of preparing coherent states on Bob's system, as shown by the decrease of Bob's volume. However, any temporal increase of the $\mathcal{QI}$ REC or the SIC indicates the violation of CP divisibility, and non-Markovianity.

relative entropy of quantum coherence for the whole system decreases monotonically, i.e.,

$$C\left(\rho_t^{AB}\right) \le C\left(\rho_s^{AB}\right),\ \forall t > s > 0. \tag{11}$$

Thus the proposed measure can effectively capture the characteristics of non-Markovianity of open quantum processes. A proof for this relation is presented in the Supplementary Information.

The above two methods can be used to effectively characterize non-Markovianity for incoherent quantum dynamics, and are the first two theoretical works on the relation between quantum coherence and non-Markovianity of a quantum process.

Non-Markovianity witness via $\mathcal{QI}$ REC and SIC

With the above theoretical background, we now present our main results, which can be applicable to general quantum dynamics. The theoretical framework is shown in Fig. 1. Considering the aforementioned bipartite system and assuming Alice will interact with her environment while Bob is kept isolated, then we have the following theorem.

- Theorem 1—In a bipartite state (Alice and Bob), assume that Alice undergoes an evolution characterized by $\{\Lambda_{t,0}\}$. Then the $\mathcal{QI}$ REC decreases monotonically if $\{\Lambda_{t,0}\}$ is CP divisible, i.e.,

$$C_r^{A|B}(\rho_t^{AB}) \le C_r^{A|B}(\rho_s^{AB}),\quad \forall t > s > 0, \tag{12}$$

where ρ_s^{AB} and ρ_t^{AB} are the states after the evolution times s and t, respectively.

The proof of this theorem is given in the Supplementary Information, using the contractivity of the relative entropy under CPTP maps and the fact that Δ^B and Λ^A commute with each other. This result demonstrates that the $\mathcal{QI}$ REC on Bob's side provides a new method for characterizing the CP divisibility of a general quantum process on Alice's side. Also the violation of the monotonic behavior of the $\mathcal{QI}$ REC indicates non-Markovianity.

An interesting observation is that the $\mathcal{QI}$ REC quantifies the upper bound for the ability of preparing coherent states on Bob's side with the assistance of Alice in the asymptotic setting. We then naturally ask whether the Markovianity on Alice's side will shrink the volume of accessible states on Bob's side, thus affecting the maximal coherence on Bob's side. We now introduce our second main result regarding the dynamical behavior of SIC during a general quantum evolution.

- Theorem 2—In the aforementioned bipartite system and assuming that Alice undergoes an evolution characterized by $\{\Lambda_{t,0}\}$. Then the SIC decreases monotonically if $\{\Lambda_{t,0}\}$ is CP divisible, i.e.,

$$\overline{C}_r^B(\rho_t^{AB}) \le \overline{C}_r^B(\rho_s^{AB}),\quad \forall t > s > 0. \tag{13}$$

A detailed proof is given in the Supplementary Information, and the main idea is as follows. We first extend Alice to an appropriate composite system of A and A', then the CPTP map Λ^A on Alice can be viewed as a unitary operation acting on both A and A'. We show that if we perform a measurement across A and A', the average coherence Bob will get is no more than what we can obtain from a local measurement on Alice, if A and A' are a product state $\rho^A \otimes \rho^{A'}$. The unitary operation does not change the maximal coherence on Bob's side, as all local measurements can be linked to performing a unitary operation followed by a measurement on a fixed basis. Then we can see that after the unitary we obtain the same maximal average coherence using a collective measurement, which is strictly greater than the coherence obtained via a local measurement on Alice. We can say that the CPTP maps on Alice's side shrink the maximal accessible coherence on Bob's side. And thus the non-monotonic behavior of the SIC indicates non-Markovianity of the quantum evolution.

Experiments

There have been several platforms for simulating[61,62] open system dynamics, such as quantum optics[63–66], trapped ions[67], and Nuclear Magnetic Resonance[68]. In our experiments, the system-environment interaction is provided by the coupling of the polarization degree (Alice, the open system) and frequency degree (environment) of Alice's photons. The experimental setup is illustrated in Fig. 2, and is constructed by three modules: (I) state preparation, (II) evolution, and (III) non-Markovianity detection.

In (I), entangled photon pairs with a central wavelength $\lambda =$ 702.2 nm can be generated via a spontaneous parametric down-conversion process (SPDC). Two interference filters with a 4-nm full width at half maximum (FWHM) are placed to filter out the proper transmission peaks. A 0.6-mm thick Fabry-Pérot cavity (FP) can be inserted into Alice's arm to change her initial environment.

In (II), the system-environment interaction takes place, which is realized by several quartz crystals. In (III), we perform quantum state tomography for detecting the related coherence-based measure. (For detailed information, see the Supplementary Information).

The purpose of our optical experiments is three-fold:

- Implementing a monotonicity test that validates our method using $\mathcal{QI}$ REC is correct even when the reference basis is changed, compared to previous ones.
- Utilizing the aforementioned method (the $\mathcal{QI}$ REC) for detecting non-Markovianity in different reference bases.
- Showing how non-Markovianity can temporally increase the ability of preparing more coherent states on Bob's side, when Bob's system is kept isolated and can only receive classical information from Alice. Moreover, the increase or decrease in the ability of creating more coherent states is coincident with entanglement and $\mathcal{QI}$ REC.

Thus we arrange our experiments in two parts. In the first part, we implement a monotonicity test. In particular, we rotate the angles of all QPs to 20°, producing a pure decoherence in the eigenbasis of $\boldsymbol{\sigma} \cdot \boldsymbol{n}_0$ on Alice, where $\boldsymbol{n}_0 = \cos 2\theta \boldsymbol{e}^X + \sin 2\theta \boldsymbol{e}^Z$ and $\theta = 20°$, showing the non-monotonic behavior of the extended coherence and the local coherence. In order to experimentally explore the dynamical behaviors of: the concurrence $E_c^{AB}(\rho_t^{AB})$, the $\mathcal{QI}$ REC $C_r^{A|B}(\rho_t^{AB})$, and the extended coherence $C_r(\rho_t^{AB})$, we

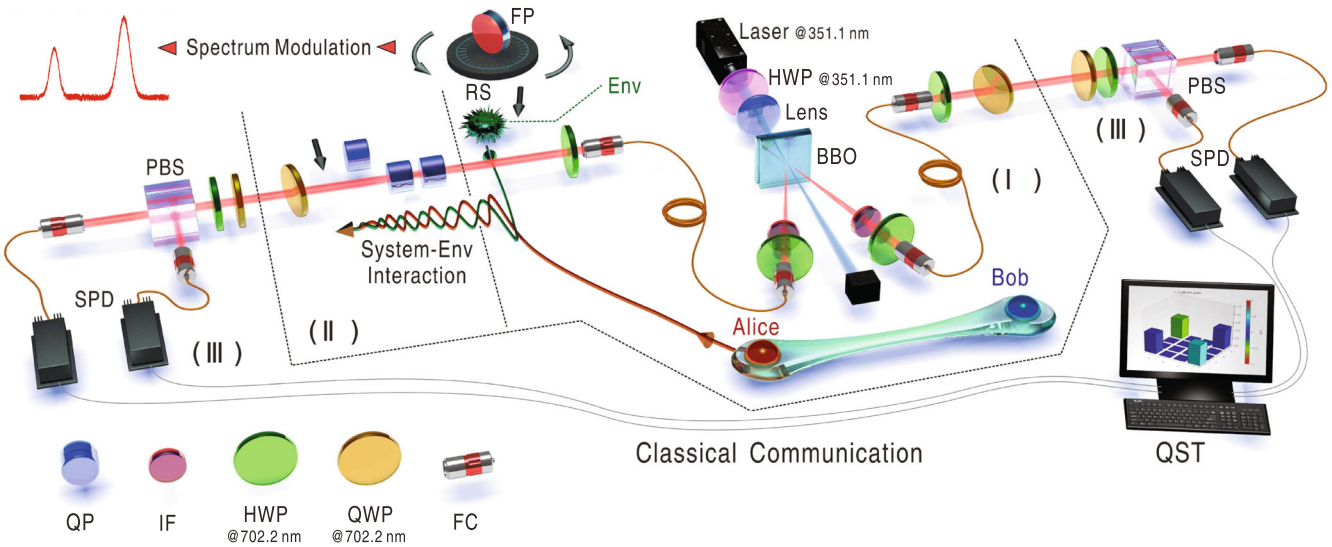

Fig. 2 The experimental setup is constructed by three modules. (I) State preparation, (II) evolution, and (III) detection. The detailed experimental setup is described in the Supplementary Information. The optical elements include: IF interference filter; HWP half-wave plate; QWP quarter-wave plate; QP quartz plate; FP Fabry-Perot cavity; BBO β-barium borate; SPD single photon detector; FC fiber coupler; PBS polarizing beam splitter; Env, environment QST, quantum state tomography.

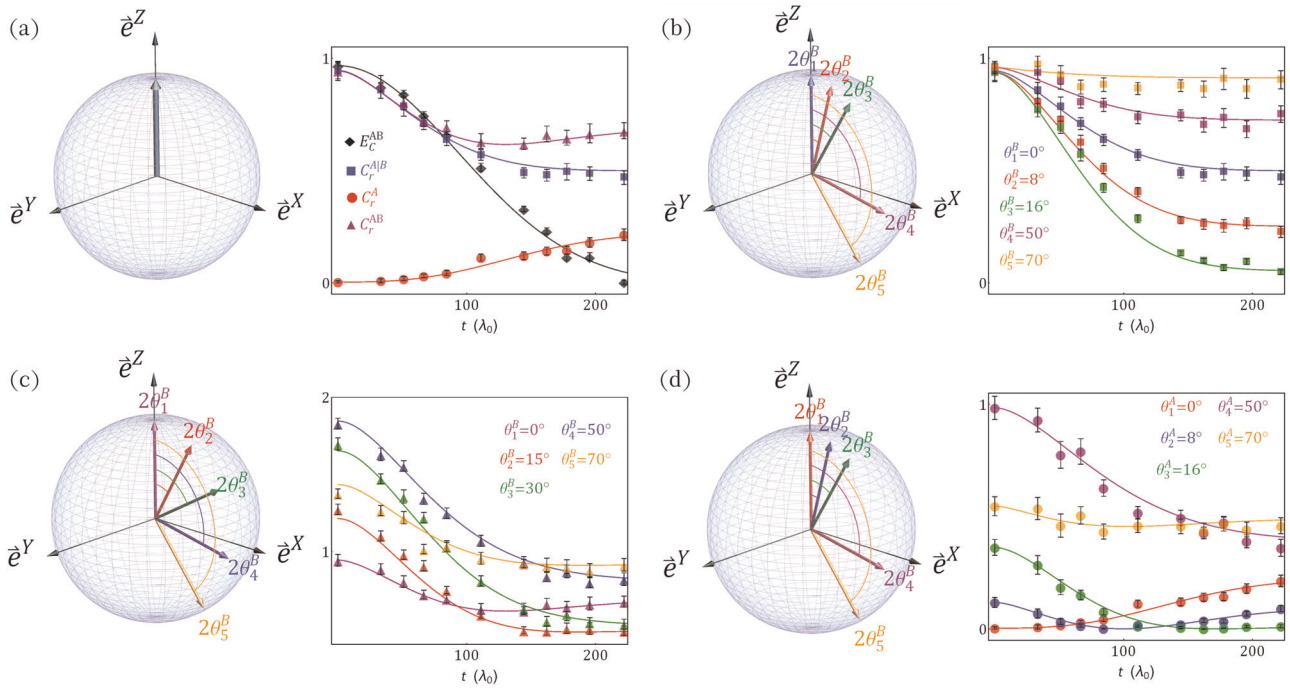

Fig. 3 Experimental results for monotonicity testing. The Markovian evolution is constructed as decoherence in the eigenbasis of $\boldsymbol{\sigma}\cdot\boldsymbol{n}_0$, where $\boldsymbol{n}_0=\cos 40^\circ \boldsymbol{e}^X+\sin 40^\circ \boldsymbol{e}^Z$ and $\boldsymbol{\sigma}=(\sigma_x,\sigma_y,\sigma_z)$. The evolution is implemented on both: a single system (Alice is prepared in $|0\rangle$) and a bipartite system (Alice and Bob share a maximally entangled state $|\phi\rangle^{AB}$). In **a**, the experimental values for the concurrence, the $\mathcal{QI}$ REC, the extended coherence (with respect to the eigenbasis of $\sigma_z^A\otimes\sigma_z^B$), and the local coherence of Alice (with respect to the σ_z^A basis) are shown as black diamonds, blue squares, purple up-triangles, and red disks, respectively. The dynamical behaviors of these coherence quantifiers are also shown with respect to different bases. The experimental values for the $\mathcal{QI}$ REC, the extended coherence, and the local coherence with respect to different bases are also calculated and shown in **b**–**d**, respectively. For the $\mathcal{QI}$ REC, we choose five reference bases as the eigenbasis of $\sigma_z^A\otimes[\boldsymbol{\sigma}\cdot\boldsymbol{n}(\theta_i^B)]$, where $\boldsymbol{n}(\theta_i^B)=\sin 2\theta_i^B\boldsymbol{e}^X+\cos 2\theta_i^B\boldsymbol{e}^Z$, and $i=1$–5. The values of θ_i^B are shown in **b**. In the right of **b**, squares in different colors show the dynamical behavior of the $\mathcal{QI}$ REC in different bases. For the extended coherence, the different reference bases are also chosen as eigenbasis of $\sigma_z^A\otimes[\boldsymbol{\sigma}\cdot\boldsymbol{n}(\theta_i^B)]$ for various θ_i^B. For the local coherence, five different bases of Alice are chosen according to the eigenbasis of $\boldsymbol{\sigma}\cdot\boldsymbol{n}(\theta_i^A)$. The choices of $\theta_i^{A(B)}$ are shown in the corresponding sub figures. All solid lines represent numerical simulations considering the fidelity of the states prepared in our laboratory, deduced assuming that the spectrum of Alice's photon is a Gaussian profile with a FWHM of 4 nm.

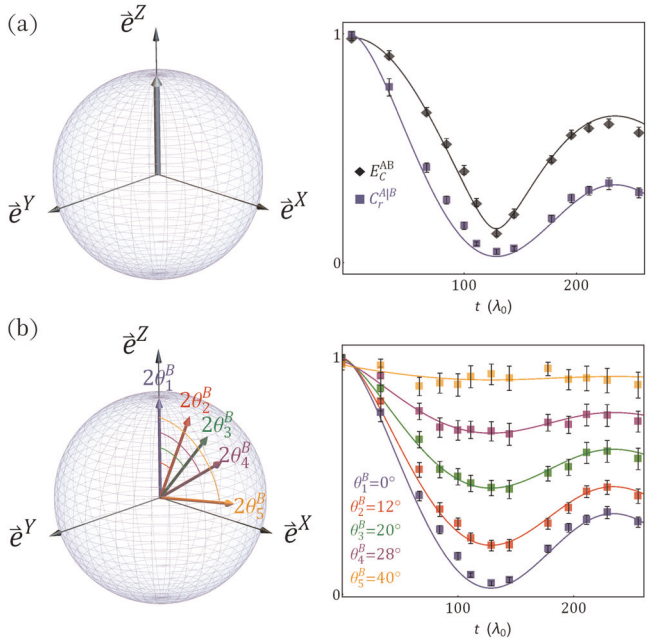

Fig. 4 Experimental results for detecting non-Markovianity via $\mathcal{QI}$ REC. The evolution is constructed as pure decoherence in the σ_z basis. The experimental values for the concurrence and the $\mathcal{QI}$ REC (with respect to the eigenbasis of $\sigma_z^A \otimes \sigma_z^B$) at different evolution times t are shown as black diamonds and blue squares in **a**. For the $\mathcal{QI}$ REC, four different bases are chosen according to the eigenbasis of $\sigma_z^A \otimes [\boldsymbol{\sigma} \cdot \boldsymbol{n}(\theta_i^B)]$ with different θ_i^B. Experimental results are shown in **b**. All solid lines represent numerical simulations considering experimental imperfections, which are deduced assuming that the spectrum of Alice's photon is a sum of two Gaussians centered at two different frequencies.

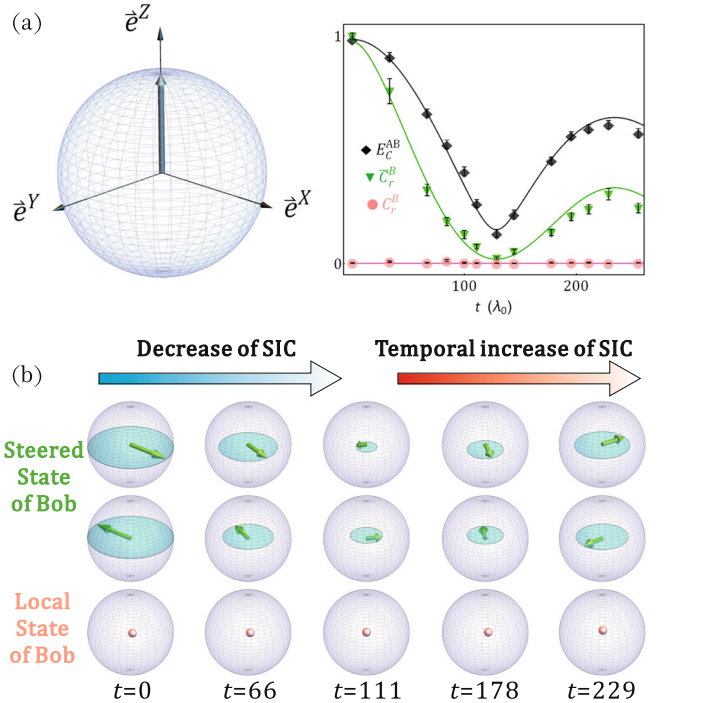

Fig. 5 Experimental results for detecting Non-Markovianity via SIC. The dynamical behavior of the SIC (in the σ_z^B basis) was also investigated under the aforementioned evolution. The experimental values are shown in **a**. In the presence of the non-Markovian decoherence noise, the optimal measurement on Alice's system is σ_x^A measurement on Alice. **b** Illustrates the dynamical behavior of the SIC with respect to the σ_z^B basis. The assisted state conversion process consists of a σ_x^A measurement and the broadcast of outcomes 0 or 1 to Bob. Bob then can prepare a more coherent state at each time t. Bob's two steered states and local states are shown as Bloch vectors in green and pink respectively, and the radius of the disks $R(t) = \sqrt{r_x(t)^2 + r_y(t)^2}$ show the coherence of each state. The experimental values for the local coherence on Bob's system are shown in **a** as pink disks.

prepared an initial state as a maximally entangled state

$$|\Phi_0\rangle = \frac{1}{\sqrt{2}}(|0\rangle^A|0\rangle^B + |1\rangle^A|1\rangle^B). \tag{14}$$

For testing the dynamical behavior of the local coherence $C_r(\rho_t^A)$, we prepare an initially incoherent pure state $|0\rangle^A$ on Alice's side, while Bob's photon is used as a trigger.

Let us now show the results of the monotonicity test first. Alice sees a spectral Gaussian as the FP is not inserted. Figure 3a illustrates the experimental dynamical behavior of these quantifiers, with respect to the $\sigma_z^A \otimes \sigma_z^B$ basis. In particular, the experimentally obtained $E_c^{AB}(\tilde{\rho}_t^{AB})$, $C_r^{A|B}(\tilde{\rho}_t^{AB})$, $C_r(\tilde{\rho}_t^{AB})$, and $C_r(\tilde{\rho}_t^A)$ at various evolution times t are shown as black diamonds, blue squares, purple up-triangles, and red disks. The tilde denotes experimentally reconstructed quantum states. These results indicate that there exists a Markovian quantum evolution in which both $C_r(\rho_t^{AB})$ and $C_r(\rho_t^A)$ behave non-monotonically, while $C_r^{A|B}(\rho_t^{AB})$ decreases monotonically. Thus both $C_r(\rho_t^{AB})$ and $C_r(\rho_t^A)$ are not suitable for characterizing Markovianity in general processes.

Figures 3b–d compare the dynamical behaviors of the aforementioned quantifiers in different bases. In particular, the experimentally obtained $C_r^{A|B}(\tilde{\rho}_t^{AB})$ in different bases with respect to the $\sigma_z^A \otimes [\boldsymbol{\sigma} \cdot \boldsymbol{n}(\theta_i^B)]$ basis are shown in (b), where the orientations of $\boldsymbol{n}(\theta_i^B)$ are shown in the Bloch representation in the left of (b), with $\theta_1^B = 0°$ (blue), $\theta_2^B = 8°$ (red), $\theta_3^B = 16°$ (green), $\theta_4^B = 50°$ (purple) and $\theta_5^B = 70°$ (orange). In (c), the experimentally obtained $C_r(\tilde{\rho}_t^{AB})$ in different bases ($\sigma_z^A \otimes [\boldsymbol{\sigma} \cdot \boldsymbol{n}(\theta_i^B)]$ basis) are shown, while this time we make different choices of θ_i^B, as shown in the plot. In (d), the $C_r(\tilde{\rho}_t^A)$ are also experimentally obtained and shown with respect to different basis ($\boldsymbol{\sigma} \cdot \boldsymbol{n}(\theta_i^A)$ basis); also the choice of θ_i^A is listed in (d). It is clear that $C_r^{A|B}(\tilde{\rho}_t^{AB})$ behaves monotonically in all the bases, during the Markovian evolution. And when $\theta^B = 0°$ or 15°, $C_r(\tilde{\rho}_t^{AB})$ will temporally increase. Non-monotonic behaviors of $C_r(\tilde{\rho}_t^A)$ can be obviously observed in our experiments in most chosen bases. In summary, the monotonicity test indicates that using only coherence (both a single system and an extended bipartite system) cannot characterize the Markovianity of a general evolution. While the behavior of the $\mathcal{QI}$ REC is monotonic and thus is suitable for characterizing Markovianity.

Let us now move to the second part of our experiments, which utilizes $\mathcal{QI}$ REC to detect non-Markovianity and show how non-Markovianity can temporally enhance the ability of preparing more coherent states on Bob's side. In particular, we implement a quantum evolution that is non-Markovian. Since either the extended coherence or the local coherence behaves non-monotonically even in a Markovian process, we do not show them in the second part of the experiments. The evolution is constructed as decoherence in the σ_z basis. We insert a FP into Alice's path, resulting in a modification of the spectrum of the frequency of Alice's photons. At different evolution times t, the values for the concurrence and the $\mathcal{QI}$ REC (with respect to different bases) are obtained. The relevant experimental values are shown as black diamonds and blue squares in Figs. 4a, b. The dynamical behaviors of $\overline{C}_r^B(\tilde{\rho}_t^{AB})$ and the local coherence of Bob $C_r^B(\tilde{\rho}_t^B)$ are also shown (in the σ_z^B basis) as green down-triangles and pink disks in Fig. 5a. And the evolution of the optimal steered

states are shown in Fig. 5b. It is clear that the non-Markovianity of a quantum evolution will temporally increase both the observed $C_r^{A|B}(\tilde{\rho}_t^{AB})$ and $\overline{C}_r^{B}(\tilde{\rho}_t^{AB})$ in our experimental protocols. The signal of non-Markovianity can be captured by $C_r^{A|B}(\tilde{\rho}_t^{AB})$ in all the basis we choose. Moreover, we experimentally show that the non-Markovianity will also temporally increase the volume of accessible states on Bob's side, resulting in an increase in the optimal steered coherence.

All solid lines represent numerical simulations also considering experimental imperfections. In the Supplementary Information, we show that the experimental results admit a theoretical analysis, and we also perform numerical simulations to show that both the $\mathcal{QI}$ REC and the SIC are applicable to a large range of quantum processes for witnessing non-Markovianity.

DISCUSSION

In this work, we theoretically provided a method for characterizing Markovianity based on the $\mathcal{QI}$ REC (between an open system and an ancilla). We experimentally investigated the evolution of the local coherence, the extended coherence, the $\mathcal{QI}$ REC, and the SIC in both Markovian and non-Markovian processes. We highlight the two-fold advantages of our method: on the one hand, it overcomes the constraint in refs. [47,48,52] as it can be applied to general quantum evolutions; on the other hand, the information carrier based on $\mathcal{QI}$ REC does not need any non-trival optimization. Moreover, in the experiments with non-Markovian processes, these results show that information backflow can enhance the ability of preparing coherent states on the ancilla system, linking non-Markovianity to the resource theory of quantum coherence.

Compared to existing methods for quantifying the degree of non-Markovinaity for a quantum process, our methods have certain advantages beyond the direct connection to quantum coherence. We also propose a potential candidate for measuring non-Markovianity based on $\mathcal{QI}$ REC, where the optimization is taken over all the bases of Bob. The Supplementary Information detail these issues.

A full understanding of these connections still remains open. Quantum coherence has been regarded as a type of resource which is more fundamental than quantum correlations, and current researches highlight the links between different quantum resources[69–71]. Though relatively elegant solutions come up in the context of coherence and correlations, a natural question arises that whether there exists a construction for the links between general quantum resources and non-Markovianity.

Another promising line of research is studying the dynamics of resource conversion processes. It has been put forward that utilizing correlated resources, together with measurement feed-forward, can be advantageous in implementing certain gates in measurement-based computation[72]. If the non-Markovianity could be related to enhancing the operational advantages of such protocols, it could imply that operational benefits can emerge when information backflow takes place.

DATA AVAILABILITY

The data sets generated and/or analyzed during this study are available from the corresponding author on reasonable request.

Received: 30 May 2019; Accepted: 7 April 2020;
Published online: 19 June 2020

REFERENCES

1. Brandão, F. G. S. L. & Gour, G. Reversible framework for quantum resource theories. *Phys. Rev. Lett.* **115**, 070503 (2015).
2. Brandão, F. G. S. L., Horodecki, M., Oppenheim, J., Renes, J. M. & Spekkens, R. W. Resource theory of quantum states out of thermal equilibrium. *Phys. Rev. Lett.* **111**, 250404 (2013).
3. Gour, G., Marvian, I. & Spekkens, R. W. Measuring the quality of a quantum reference frame: The relative entropy of frameness. *Phys. Rev. A* **80**, 012307 (2009).
4. Lostaglio, M., Korzekwa, K., Jennings, D. & Rudolph, T. Quantum coherence, time-translation symmetry, and thermodynamics. *Phys. Rev. X* **5**, 021001 (2015).
5. Marvian, I. & Spekkens, R. W. Extending noethers theorem by quantifying the asymmetry of quantum states. *Nat. Commun.* **5**, 3821 (2014).
6. Baumgratz, T., Cramer, M. & Plenio, M. B. Quantifying coherence. *Phys. Rev. Lett.* **113**, 140401 (2014).
7. Girolami, D. Observable measure of quantum coherence in finite dimensional systems. *Phys. Rev. Lett.* **113**, 170401 (2014).
8. Streltsov, A., Adesso, G. & Plenio, M. B. Colloquium: quantum coherence as a resource. *Rev. Mod. Phys.* **89**, 041003 (2017).
9. Streltsov, A., Singh, U., Dhar, H. S., Bera, M. N. & Adesso, G. Measuring quantum coherence with entanglement. *Phys. Rev. Lett.* **115**, 020403 (2015).
10. Winter, A. & Yang, D. Operational resource theory of coherence. *Phys. Rev. Lett.* **116**, 120404 (2016).
11. Yuan, X., Zhou, H., Cao, Z. & Ma, X. Intrinsic randomness as a measure of quantum coherence. *Phys. Rev. A* **92**, 022124 (2015).
12. Bromley, T. R., Cianciaruso, M. & Adesso, G. Frozen quantum coherence. *Phys. Rev. Lett.* **114**, 210401 (2015).
13. Huang, Z. & Situ, H. Non-Markovian dynamics of quantum coherence of two-level system driven by classical field. *Quantum Inf. Process.* **16**, 222 (2017).
14. Lostaglio, M., Korzekwa, K. & Milne, A. Markovian evolution of quantum coherence under symmetric dynamics. *Phys. Rev. A* **96**, 032109 (2017).
15. Man, Z.-X., Xia, Y.-J. & Franco, R. L. Cavity-based architecture to preserve quantum coherence and entanglement. *Sci. Rep.* **5**, 13843 (2015).
16. Qin, M., Ren, Z. & Zhang, X. Dynamics of quantum coherence and quantum phase transitions in x y spin systems. *Phys. Rev. A* **98**, 012303 (2018).
17. Silva, I. A., Souza, A. M., Bromley, T. R., Cianciaruso, M. & Marx, R. Observation of time-invariant coherence in a nuclear magnetic resonance quantum simulator. *Phys. Rev. Lett.* **117**, 160402 (2016).
18. Breuer, H.-P. & Petruccione, F. *The Theory of Open Quantum Systems*. (Oxford University Press on Demand, 2002).
19. Chen, H.-B., Lambert, N., Cheng, Y.-C., Chen, Y.-N. & Nori, F. Using non-Markovian measures to evaluate quantum master equations for photosynthesis. *Sci. Rep.* **5**, 12753 (2015).
20. Chen, Y.-N., Chen, G.-Y., Liao, Y.-Y., Lambert, N. & Nori, F. Detecting non-Markovian plasmonic band gaps in quantum dots using electron transport. *Phys. Rev. B* **79**, 245312 (2009).
21. Li, L., Hall, M. J. & Wiseman, H. M. Concepts of quantum non-markovianity: a hierarchy. *Phys. Rep.* **759**, 1–51 (2018).
22. Pollock, F. A., Rodríguez-Rosario, C., Frauenheim, T., Paternostro, M. & Modi, K. Operational Markov condition for quantum processes. *Phys. Rev. Lett.* **120**, 040405 (2018).
23. Weiss, U. *Quantum Dissipative Systems13*. (World scientific, 2012).
24. Xiong, H.-N., Lo, P.-Y., Zhang, W.-M. & Nori, F. Non-Markovian complexity in the quantum-to-classical transition. *Sci. Rep.* **5**, 13353 (2015).
25. Yin, X., Ma, J., Wang, X. & Nori, F. Spin squeezing under non-Markovian channels by the hierarchy equation method. *Phys. Rev. A* **86**, 012308 (2012).
26. Zhang, J., Liu, Y.-X., Wu, R.-B., Jacobs, K. & Nori, F. Non-Markovian quantum input-output networks. *Phys. Rev. A* **87**, 032117 (2013).
27. Zhang, W.-M., Lo, P.-Y., Xiong, H.-N., Tu, M. W.-Y. & Nori, F. General non-Markovian dynamics of open quantum systems. *Phys. Rev. Lett.* **109**, 170402 (2012).
28. Gorini, V., Kossakowski, A. & Sudarshan, E. C. G. Completely positive dynamical semigroups of n-level systems. *J. Math. Phys.* **17**, 821–825 (1976).
29. Lindblad, G. On the generators of quantum dynamical semigroups. *Commun. Math. Phys.* **48**, 119–130 (1976).
30. Breuer, H.-P., Laine, E.-M. & Piilo, J. Measure for the degree of non-Markovian behavior of quantum processes in open systems. *Phys. Rev. Lett.* **103**, 210401 (2009).
31. Bae, J. & Chruściński, D. Operational characterization of divisibility of dynamical maps. *Phys. Rev. Lett.* **117**, 050403 (2016).
32. Bylicka, B., Chruściński, D. & Maniscalco, S. Non-Markovianity and reservoir memory of quantum channels: a quantum information theory perspective. *Sci. Rep.* **4**, 5720 (2014).
33. Chen, S.-L. et al. Quantifying non-Markovianity with temporal steering. *Phys. Rev. Lett.* **116**, 020503 (2016).
34. Ku, H.-Y. et al. Temporal steering in four dimensions with applications to coupled qubits and magnetoreception. *Phys. Rev. A* **94**, 062126 (2016).
35. Li, C.-M., Chen, Y.-N., Lambert, N., Chiu, C.-Y. & Nori, F. Certifying single-system steering for quantum-information processing. *Phys. Rev. A* **92**, 062310 (2015).

36. Lorenzo, S., Plastina, F. & Paternostro, M. Geometrical characterization of non-Markovianity. *Phys. Rev. A* **88**, 020102 (2013).
37. Lu, X.-M., Wang, X. & Sun, C. P. Quantum fisher information flow and non-Markovian processes of open systems. *Phys. Rev. A* **82**, 042103 (2010).
38. Luo, S., Fu, S. & Song, H. Quantifying non-Markovianity via correlations. *Phys. Rev. A* **86**, 044101 (2012).
39. Rajagopal, A. K., Usha Devi, A. R. & Rendell, R. W. Kraus representation of quantum evolution and fidelity as manifestations of Markovian and non-Markovian forms. *Phys. Rev. A* **82**, 042107 (2010).
40. Rivas, A., Huelga, S. F. & Plenio, M. B. Entanglement and non-Markovianity of quantum evolutions. *Phys. Rev. Lett.* **105**, 050403 (2010).
41. Song, H., Luo, S. & Hong, Y. Quantum non-Markovianity based on the fisher-information matrix. *Phys. Rev. A* **91**, 042110 (2015).
42. Strathearn, A., Kirton, P., Kilda, D., Keeling, J. & Lovett, B. W. Efficient non-Markovian quantum dynamics using time-evolving matrix product operators. *Nat. Commun.* **9**, 3322 (2018).
43. Xiong, S.-J., Zhang, Y., Sun, Z., Yu, L. & Su, Q. Experimental simulation of a quantum channel without the rotating-wave approximation: testing quantum temporal steering. *Optica* **4**, 1065–1072 (2017).
44. Addis, C., Brebner, G., Haikka, P. & Maniscalco, S. Coherence trapping and information backflow in dephasing qubits. *Phys. Rev. A.* **89**, 024101 (2014).
45. Bhattacharya, S., Banerjee, S. & Pati, A.K. Evolution of coherence and non-classicality underglobal environmental interaction. *Quantum Inf Process* **17**, 236 (2018).
46. Cakmak, B., Pezzutto, M., Paternostro, M. & Mustecaplioglu, O. Non-Markovianity, coherence, and system-environment correlations in a long-range collision model. *Phys. Rev. A* **96**, 022109 (2017).
47. Chanda, T. & Bhattacharya, S. Delineating incoherent non-Markovian dynamics using quantum coherence. *Ann. Phys.* **366**, 1–12 (2016).
48. He, Z., Zeng, H.-S., Li, Y., Wang, Q. & Yao, C. Non-Markovianity measure based on the relative entropy of coherence in an extended space. *Phys. Rev. A* **96**, 022106 (2017).
49. Liu, Y., Zou, H.-M. & Fang, M.-F. Quantum coherence and non-Markovianity of atom in dissipative cavity under weak measurement. *Phys. B* **27**(1), 010304 (2018).
50. Man, Z.-X., Xia, Y.-J. & Franco, R. L. Temperature effects on quantum non-Markovianity via collision models. *Phys. Rev. A* **97**, 062104 (2018).
51. Mirafzali, S. Y. & Baghshahi, H. R. Non-Markovianity detection with coherence measures based on the tsallis relative α entropies. *Phys. A: Stat. Mech. Appl.* **514**, 274–279 (2019).
52. Passos, M. et al. Non-markovianity through quantum coherence in an all-optical setup. *Opt. Lett.* **44**, 2478–2481 (2019).
53. Radhakrishnan, C., Chen, P., Jambulingam, S., Byrnes, T. & Ali, M. M. Time dynamics of quantum coherence and monogamy in a non-Markovian environment. *Sci Rep* **9**, 2363 (2019).
54. Zhang, Y.-J., Han, W., Xia, Y.-J., Yu, Y.-M. & Fan, H. Role of initial system-bath correlation on coherence trapping. *Sci. Rep.* **5**, 13359 (2015).
55. Chitambar, E. et al. Assisted distillation of quantum coherence. *Phys. Rev. Lett.* **116**, 070402 (2016).
56. Hu, X. & Fan, H. Extracting quantum coherence via steering. *Sci. Rep.* **6**, 34380 (2016).
57. Hu, X., Milne, A., Zhang, B. & Fan, H. Quantum coherence of steered states. *Sci. Rep.* **6**, 19365 (2016).
58. Vedral, V. The role of relative entropy in quantum information theory. *Rev. Mod. Phys.* **74**, 197 (2002).
59. Streltsov, A., Rana, S., Bera, M. N. & Lewenstein, M. Towards resource theory of coherence in distributed scenarios. *Phys. Rev. X* **7**, 011024 (2017).
60. Wu, K-D., Theurer, T., Xiang, G-Y., Li, C-F., Guo, G-C., Plenio, M. B. & Streltsov, A. Quantum coherence and state conversion: theory and experiment. *npj Quantum Inf* **6**, 22 (2020).
61. Buluta, I. & Nori, F. Quantum simulators. *Science* **326**, 108–111 (2009).
62. Georgescu, I. M., Ashhab, S. & Nori, F. Quantum simulation. *Rev. Mod. Phys.* **86**, 153–185 (2014).
63. Bernardes, N. K. et al. Experimental observation of weak non-markovianity. *Sci. Rep.* **5**, 17520 (2015).
64. Cialdi, S. et al. All-optical quantum simulator of qubit noisy channels. *Appl. Phys. Lett.* **110**, 081107 (2017).
65. Cuevas, Á., Geraldi, A., Liorni, C., Bonavena, L. D. & De Pasquale, A. All-optical implementation of collision-based evolutions of open quantum systems. *Sci. Rep.* **9**, 3205 (2019).
66. Liu, B.-H. et al. Experimental control of the transition from Markovian to non-Markovian dynamics of open quantum systems. *Nat. Phys.* **7**, 931–934 (2011).
67. Wittemer, M., Clos, G., Breuer, H.-P., Warring, U. & Schaetz, T. Measurement of quantum memory effects and its fundamental limitations. *Phys. Rev. A* **97**, 020102 (2018).
68. Bernardes, N. K., Peterson, J. P., Sarthour, R. S., Souza, A. M. & Monken, C. High resolution non-markovianity in nmr. *Sci. Rep.* **6**, 33945 (2016).
69. Ma, J., Yadin, B., Girolami, D., Vedral, V. & Gu, M. Converting coherence to quantum correlations. *Phys. Rev. Lett.* **116**, 160407 (2016).
70. Streltsov, A., Singh, U., Dhar, H. S., Bera, M. N. & Adesso, G. Measuring quantum coherence with entanglement. *Phys. Rev. Lett.* **115**, 020403 (2015).
71. Wu, K.-D., Hou, Z., Zhao, Y.-Y., Xiang, G.-Y. & Li, C.-F. Experimental cyclic interconversion between coherence and quantum correlations. *Phys. Rev. Lett.* **121**, 050401 (2018).
72. Raussendorf, R. & Briegel, H. J. A one-way quantum computer. *Phys. Rev. Lett.* **86**, 5188–5191 (2001).

ACKNOWLEDGEMENTS

The work at USTC is supported by the National Natural Science Foundation of China under Grants (Nos. 11574291, 11774334, and 61828303), the National Key Research and Development Program of China (No.2017YFA0304100), Key Research Program of Frontier Sciences, CAS (No. QYZDY-SSW-SLH003), National Key R & D Program (2016YFA0301700), and Anhui Initiative in Quantum Information Technologies. D.D. acknowledges partial support by the Australian Research Council's Discovery Projects Funding Scheme under Project DP190101566 and the U.S. Office of Naval Research Global under Grant N62909-19-1-2129. F.N. is supported in part by: NTT Research, Army Research Office (ARO) (Grant No. W911NF-18-1-0358), Japan Science and Technology Agency (JST) (via the CREST Grant No. JPMJCR1676), Japan Society for the Promotion of Science (JSPS) (via the KAKENHI Grant No. JP20H00134, and the JSPS-RFBR Grant No. JPJSBP120194828), and the Grant No. FQXi-IAF19-06 from the Foundational Questions Institute Fund (FQXi), a donor advised fund of the Silicon Valley Community Foundation.

AUTHOR CONTRIBUTIONS

G.Y.X. conceived and supervised the project. K.D.W. designed the theoretical protocol, and implemented the experiments with assistance from Z.H. and G.Y.X. K.D.W. analyzed the experimental data with the help of G.Y.X., C.F.L., G.C.G., D.D. and F.N. K.D.W., G.Y.X., D.D. and F.N. wrote the paper with contributions from all authors.

COMPETING INTERESTS

The authors declare no competing interests.

ADDITIONAL INFORMATION

Supplementary information is available for this paper at https://doi.org/10.1038/s41534-020-0283-3.

Correspondence and requests for materials should be addressed to G.-Y.X.

Reprints and permission information is available at http://www.nature.com/reprints

Publisher's note Springer Nature remains neutral with regard to jurisdictional claims in published maps and institutional affiliations.